Complement-Induced Cell Death by Rituximab Depends on CD20 Expression Level and Acts Complementary to Antibody-Dependent Cellular Cytotoxicity

Tom van Meerten, Rozemarijn S. van Rijn, Samantha Hol, Anton Hagenbeek, and Saskia B. Ebeling

Abstract

Purpose: The use of the CD20-specific antibody rituximab has greatly improved the response to treatment of CD20$^+$ follicular lymphoma. Despite the success of rituximab, resistance has been reported and prognostic markers to predict individual response are lacking. The level of CD20 expression on tumors has been related to response, but results of several studies are contradictory and no clear relationship could be established. Complement-dependent cytotoxicity (CDC) and antibody-dependent cellular cytotoxicity (ADCC) are thought to be important effector mechanisms, but the exact mechanism of rituximab-mediated cell kill is still unknown. Importantly, no data have been reported on the combined contribution of CDC and ADCC.

Experimental Design: We have developed a system of clonally related CEM-CD20 cells by retroviral transfer of the human CD20 cDNA ($n = 90$). This set of cells, with the CD20 molecule as the only variable, was used to study the importance of CD20 expression level on rituximab-mediated CDC, ADCC, and the combination.

Results: We show a sigmoidal correlation of CD20 expression level and rituximab-mediated killing via CDC but not ADCC. On both high and low CD20-expressing cells, all CD20 molecules were translocated into lipid rafts after rituximab binding. Furthermore, CDC and ADCC act simultaneously and CDC-resistant cells are sensitive to ADCC and vice versa.

Conclusions: These findings suggest that CDC depends on CD20 expression level and that both CDC and ADCC act complementary. These data give new insights into novel strategies to improve the efficacy of CD20-specific antibodies for the treatment of CD20$^+$ tumors.

The CD20-specific monoclonal antibody (mAb) rituximab has been widely proven to be a successful treatment of a variety of B-cell malignancies and B-cell-related diseases (1, 2). However, resistance against rituximab occurs and there is no prognostic marker to predict individual response (3–5).

Various *in vitro* and *in vivo* experiments have shown that elimination of CD20$^+$ cells is effected by the IgG1 chain of rituximab, which triggers complement-dependent cytotoxicity (CDC), and induces the recruitment of effector cells, leading to antibody-dependent cellular cytotoxicity (ADCC; refs. 6–13). On the other hand, the complement regulatory proteins (CRP)

CD46, CD55, and CD59 have been shown to inhibit rituximab-mediated cell kill by interfering with complement activation (10, 11, 13). However, despite these current understandings, the exact mechanism of rituximab-mediated cell kill is still unknown. Importantly, no data have been reported on the combined contribution of CDC and ADCC. Consequently, the differential susceptibility of CD20-expressing tumors to rituximab is incompletely understood.

In general, follicular lymphoma cells can be killed effectively by rituximab, whereas B-cell chronic lymphocytic leukemia (CLL) cells show a poor response. A major difference between these cell types is the higher level of CD20 expression on follicular lymphoma cells compared with B-cell CLL cells (7, 11, 14). This suggests that rituximab sensitivity depends on CD20 expression. Therefore, several studies have addressed the question whether the CD20 expression level may be used to predict progression of disease and response to treatment (5, 10–13). The results are conflicting. *In vitro* analysis of follicular lymphoma cells revealed no correlation between CD20 expression level and CDC sensitivity (10, 12). In another study, rituximab-mediated CDC *in vitro* did not correlate with clinical response (13). In a comparison of B-cell CLL samples, no significant correlation was found between CD20 expression level and rituximab response *in vivo* (5). In contrast, a marked correlation was reported in two other studies involving a variety of B-cell malignancies (7, 11). This significant variability in the reported sensitivity to rituximab-mediated CDC among B-cell lines and primary tumor samples may have been affected
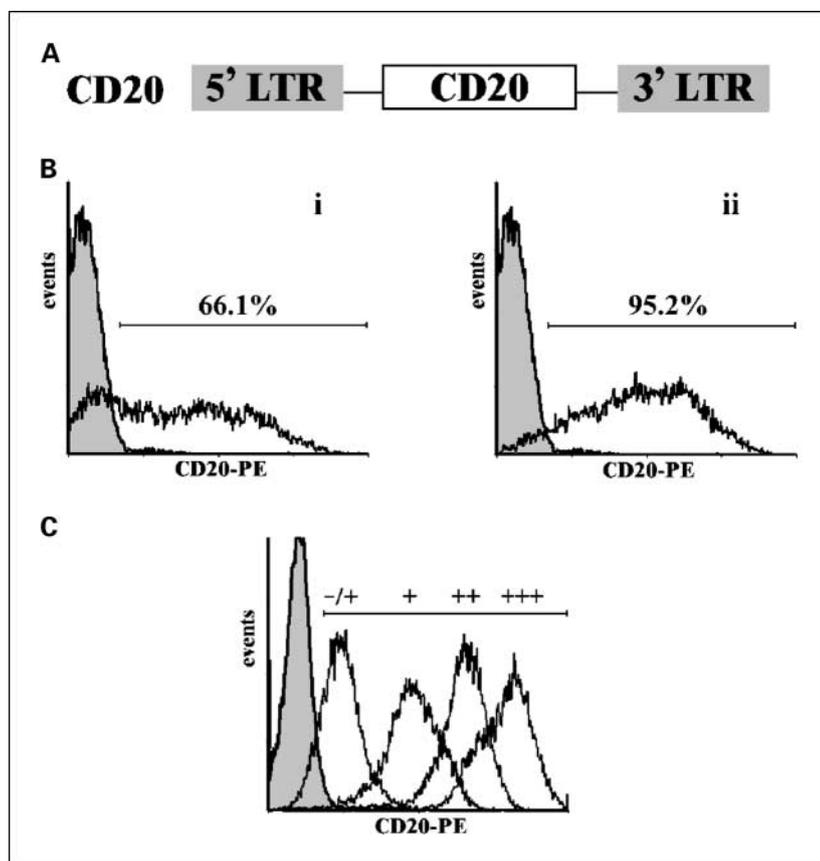
Fig. 1. CD20 transduction of CEM T cells. *A,* CD20-encoding retroviral vector. *LTR,* long terminal repeat. *B,* fluorescence-activated cell sorting analysis of transduced (*i*) and purified (*ii*) CD20$^+$ CEM cells. *C,* examples of the CEM-CD20 transgenic clones, with low (−/+), low-intermediate (+), high-intermediate (++), and high (+++) CD20 expression profiles.

by biological variables other than CD20 expression level. Moreover, within primary tumor samples, not all cells may express CD20 (11).

To unequivocally define the role of CD20 expression level in rituximab-mediated killing, a controlled experimental setting is required, in which CD20 expression level is the only variable. Importantly, the relationship between CD20 expression level and the combined activity of CDC and ADCC requires investigation.

In this study, we present a unique experimental model consisting of a set of clonally related CD20$^+$ transgenic cells that collectively cover a wide spectrum of CD20 expression levels. Using this model, we investigated the relationship between CD20 expression level and rituximab-mediated cell kill and the separate and combined contribution of CDC and ADCC. Our results show that rituximab-induced CDC, but not ADCC, clearly depends on the CD20 expression level. Moreover, we show that the activity of rituximab significantly increases when CDC and ADCC act simultaneously. Importantly, we found that CDC-resistant cells are still susceptible to ADCC and vice versa, which leads us to conclude that these effector mechanisms act complementary.

Materials and Methods

Generation of CD20$^+$ CEM cells. The human CD20 cDNA was amplified by PCR from the pCMV-CD20 expression vector by using the following primers: CD20-FW 5′-GGGCCGCGGCCGCCGCCATGACAA-CACCCAGAAATTCAGTA-3′ and CD20-*Sal*I RV 5′-GGGG*TCGAC*AAAT-

TCACTTAAGGAGAGCTGTCAT-3′ (15). The amplified CD20 fragment was ligated into a pCRII TOPO cloning vector (Invitrogen, Paisley, United Kingdom), according to the manufacturer′s instructions, resulting in the pCRII-CD20 vector. The CD20 cDNA was released from the pCRII-CD20 vector with *Bam*HI and *Sal*I endonuclease restriction enzymes. The CD20 cDNA was then inserted into the *Bam*HI and *Sal*I sites of the pMX retroviral vector (16). Generation of virus particles, transduction of the CEM and Jurkat CD20$^-$ T-cell lines, and purification of CD20$^+$ cells with paramagnetic beads was done as described previously (17, 18). Clonal CEM-CD20 and Jurkat-CD20 cells were generated by limiting dilution culture of the selected cells in a 96-well flat-bottomed tissue culture plate (Nunc, Roskilde, Denmark).

Cells and cell culture. The CEM T-cell line, Jurkat T-cell line, and Raji lymphoma cells (18) were cultured in culture medium consisting of RPMI (Life Technologies, Paisley, Scotland), 10% FCS (Integro, Zaandam, the Netherlands), 100 units/mL penicillin and 100 μg/mL streptomycin (Life Technologies), and 5×10^{-5} mol/L 2-mercaptoe-thanol (Merck, Darmstadt, Germany). Peripheral blood mononuclear cells were isolated by density centrifugation through Ficoll (Amersham Pharmacia, Uppsala, Sweden) and stimulated with 300 units/mL human recombinant interleukin (IL)-2 (Proleukin, Chiron, Amsterdam, the Netherlands) and IL-12 (Peprotech, London, United Kingdom) for 24 hours. All cells were cultured at 37°C in a 5% CO_2 atmosphere. CLL (6×) and lymphomas (6×) were stored in liquid nitrogen. On thawing, they were used directly to determine the absolute number of CD20 molecules per cell and compared with the clonal CD20 transgenic cells.

Flow cytometric analysis. Expression of CD20 and CRPs was determined by fluorescence-activated cell sorting (Becton Dickinson, Mountain View, CA). Antibodies used were anti-CD20-phycoerythrin (PE; BD Biosciences, San Jose, CA), anti-CD46-phycoerythrin (Immunotech, Marseilles, France), and anti-CD55-phycoerythrin and

anti-CD59-phycoerythrin (CLB, Amsterdam, the Netherlands). Rituximab was obtained from Roche (Basel, Switzerland). The absolute numbers of CD20 molecules per cell were determined with Quanti-BRITE CD20 PE (Becton Dickinson, San Jose, CA) kit according to the manufacturer's instructions. The antibodies bound per cell (ABC) represent the absolute number of CD20 molecules per cell.

Measurement of raft-associated antigen by Triton X-100 insolubility. To study the presence of CD20 in cholesterol-rich microdomains before and after rituximab ligation, we used a rapid flow cytometry method based on Triton X-100 insolubility at low temperatures as described previously (19). Briefly, cells were washed in PBS and resuspended at 2.5×10^6/mL. Cells were incubated with 10 μg/mL rituximab or control anti-CD7-FITC mAb (Becton Dickinson, Mountain View, CA) for 15 minutes at 37°C. Next, the samples were washed in cold PBS and then divided in half. One half was maintained on ice and stained later with rituximab to calculate the 100% surface antigen expression. The other half was treated with 0.5% Triton X-100 for 15 minutes on ice to determine the proportion of antigens remaining in the Triton X-100 (Riedel de Haen, Seelze, Germany) insoluble fraction. Cell fragments were spun down and the pellet, containing the lipid rafts, was stained with rituximab. Next, the rituximab-ligated pellet of the Triton X-100–treated and nontreated cells was stained with anti-human IgG1-FITC antibody. The mean fluorescence intensity (MFI) was determined by fluorescence-activated cell sorting as described above.

Rituximab-mediated cytotoxicity assays. For CDC assays, 1×10^6 cells were resuspended in 500 μL human serum and 500 μL culture medium with or without 10 μg/mL rituximab at 37°C for 30 minutes. Dead and viable cells were discriminated by addition of 1 μg/mL propidium iodide (PI). Measurement of ADCC and the combination

of ADCC and CDC was based on a recently described fluorescence-activated cell sorting–based assay (20). In brief, CD20+ cells were washed in PBS and resuspended at 1×10^6/mL. Next, the cells were stained with 5 μmol/L carboxyfluorescein diacetate succinimidyl ester (CFSE; Molecular Probes Europe BV, Leiden, the Netherlands) for 10 minutes at 37°C. The reaction was stopped by adding an equal volume of FCS. Cells were washed twice with PBS and 2,500 cells per well were plated in a 96-well round-bottomed microtiter plate (Nunc) in the absence or presence of 10 μg/mL rituximab. Stimulated peripheral blood mononuclear cells were added at 1:10 target/effector ratio without (ADCC) or with (ADCC + CDC) human serum (50%). The optimal conditions for rituximab-mediated ADCC to obtain maximum cell kill have been determined previously (21). After incubating the plates for 4 hours at 37°C, the cells were harvested and 1 μg/mL PI and 5,000 Flow Count Fluorospheres (Coulter Corp., Miami, FL) were added. To determine the absolute number of surviving cells, data acquisition was stopped after measurement of 2,500 fluorospheres and the CFSE+ and PI− cells were counted. The fraction of rituximab-mediated cell kill was calculated as follows:

$$\% \text{ Rituximab survival} = \frac{+\text{RTX absolute no. viable CFSE}^+ \text{ PI}^- \text{ cells}}{-\text{RTX absolute no. viable CFSE}^+ \text{ PI}^- \text{ cells}} \times 100$$

in which +RTX absolute no. viable CFSE+ PI− cells represents the absolute number of CFSE+ PI− cells after rituximab treatment and −RTX absolute no. viable CFSE+ PI− cells represents the absolute number of CFSE+ PI− cells without rituximab treatment.

Statistical analysis. Sigmoidal dose-response equation or linear regression was used to compare the rituximab-mediated CDC and

Fig. 2. Rituximab-mediated CDC and ADCC assays on CEM-CD20 clones. *A,* MFI of individual CD20-expressing CEM clones ($n = 90$). *B,* range of CD20 and CRP (CD46, CD55, and CD59) expression of CEM-CD20 clones ($n = 12$). Clones were selected that covered a wide range of CD20 expression. *C,* relationship between the level of CD20 expression and CDC-mediated cell kill in the presence of rituximab and human serum. The MFI of CD20 expression level of individual CEM-CD20 clones was determined and plotted against the fraction of cell death induced by rituximab and human serum. Experiments were done in duplicate. *D,* relationship between the level of CD20 expression and CDC-mediated cell kill in the presence of rituximab and human serum. The MFI of CD20 expression level of individual Jurkat-CD20 clones was determined and plotted against the fraction of cell death induced by rituximab and human serum. Experiments were done in duplicate. *E,* CEM-CD20 cells were incubated with 10 μg/mL rituximab or anti-CD7 and the samples were divided in half. *White columns,* directly stained with anti-IgG1-FITC; *hatched columns,* first treated with Triton X-100 and then stained with anti-IgG1-FITC; *black columns,* percentage CDC of the clones in the presence of rituximab and serum as described previously. Experiments are done in duplicate. *F,* relationship between the CD20 expression level and ADCC-mediated cell death in the presence of rituximab. The CD20-MFI was plotted against the % ADCC after incubation with effector cells and rituximab. Experiments were done in triplicate. *Points,* mean; *bars,* SD.
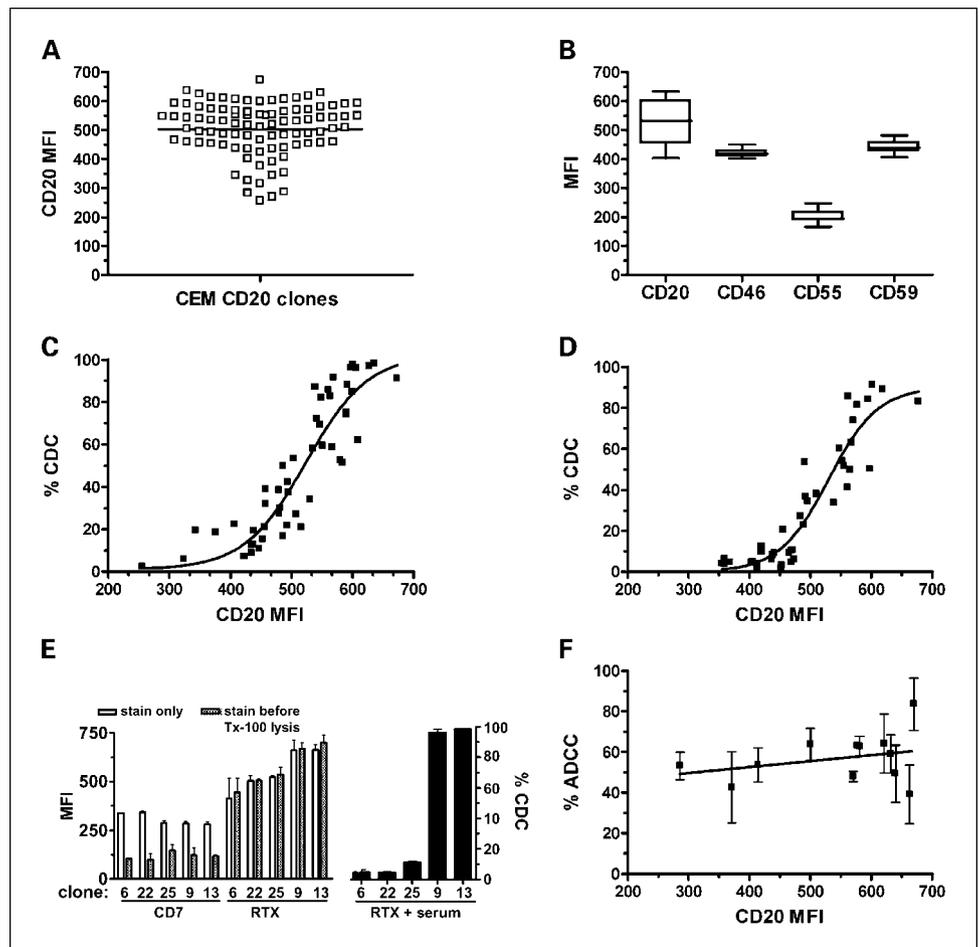
ADCC versus CD20 expression level by using SPSS 11.5 or GraphPad Prism 4.0 software. A two-way ANOVA test was used to show the significance of CDC and ADCC compared with the combined activity. Three or four replicate killing assays per clone were averaged, and the mean and SD were calculated and used for statistical comparison.

Results

To define the effect of CD20 expression level on rituximab-mediated cell kill, a system is required in which the CD20 molecule is the only variable. To obtain such a system, we chose to generate CD20^{+} clones of the CD20^{−} T-cell lines CEM and Jurkat. This collection of clones, expressing variable levels of the CD20 molecule, was then used to evaluate rituximab-induced cytotoxicity. For stable expression of the CD20 molecule on CD20^{−} cells, we constructed a CD20-encoding retroviral vector (Fig. 1A). After transduction, CD20^{+} cells were selected with CD20 antibody-conjugated paramagnetic beads and were purified to >95% homogeneity (Fig. 1B). To obtain a panel of CD20^{+} cells with different intensities of CD20 expression, we generated CD20 transgenic clones by limiting dilution culture of the purified cells. Figure 1C shows an example of the diversity in CD20 expression level of the CEM-CD20 transgenic clones with low, low-intermediate, high-intermediate, and high CD20 expression profiles. Figure 2A shows the MFI of the CD20 expression level of all clones. The MFI of individual CD20^{+} clones ranged from 256 to 693 with a mean MFI of 505 (n = 90). Twelve clones were selected that cover a wide range of CD20 expression levels and the level of expression of CRPs was determined. As shown in Fig. 2B, a similar expression level of CD46, CD55, and CD59 was observed in all clones (MFI of 421 ± 17, 201 ± 22, and 441 ± 24, respectively). The same results were obtained with transduced CD20^{+} Jurkat clones (data not shown). This collection of clones provided a unique set up to analyze the effect of the CD20 expression level on rituximab-mediated killing by both CDC and ADCC.

First, 50 CEM-CD20 clones with low, intermediate, and high CD20 expression levels and the nontransduced CEM cells were subjected to rituximab-induced CDC. Figure 2C displays the correlation between CD20 expression level, indicated by the MFI of CD20 expression, and rituximab-mediated CDC. A minimum CD20 MFI of ∼450 was required to induce rituximab-specific CDC. Maximum CDC was obtained with a MFI of >600. These data show a significant correlation between the CD20 expression level and rituximab-induced CDC (r^2 = 0.83; n = 51). Similar results were obtained with CD20 transgenic Jurkat clones as shown in Fig. 2D (r^2 = 0.88; n = 42).

Induction of CDC by rituximab is dependent on the translocation of CD20 into Triton X-100–insoluble cholesterol-rich microdomains (lipid rafts; ref. 19). Therefore, we addressed the question whether the low level of CDC at low CD20 expression was associated with incomplete translocation of CD20 into lipid rafts after rituximab ligation.

Figure 2E shows the redistribution of CD20 into lipid rafts after rituximab binding of five different clones with different CD20 expression levels. In all clones, CD20 was completely reorganized in the plasma membrane after binding with rituximab independent of the number of CD20 molecules expressed. No significant amount of CD20 antigen was detected
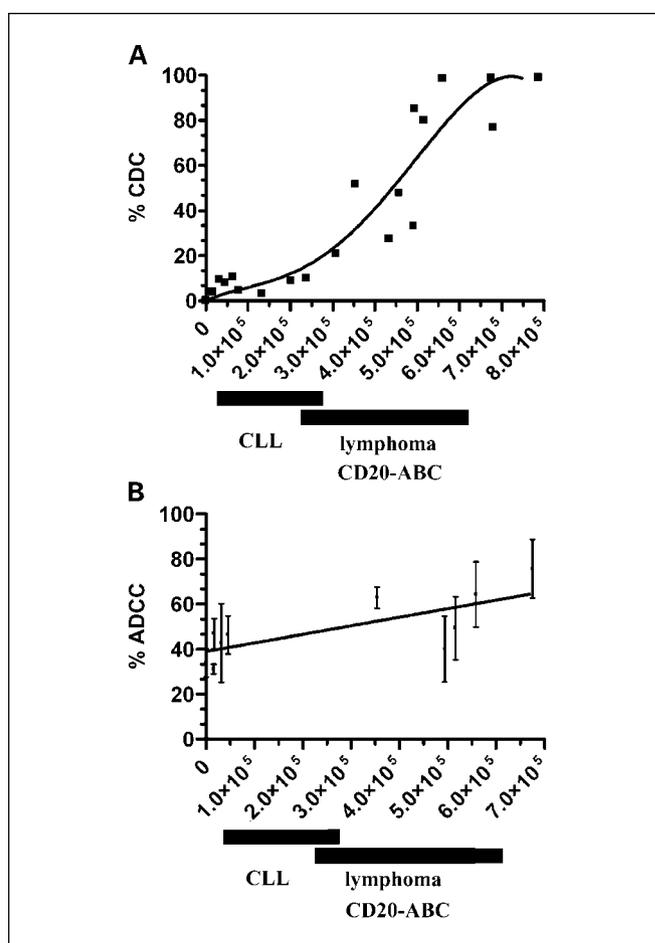

Fig. 3. Correlation of CD20-ABC and rituximab-mediated CDC and ADCC assays on CEM-CD20 clones. The absolute numbers (ABC) of CD20 molecules of individual CEM-CD20 clones were determined and plotted against the extent of CDC (*A*) or ADCC (*B*). *Points,* CD20-ABC of CLL and lymphoma samples.

in rafts before rituximab binding and hyper-cross-linking of rituximab by anti-human IgG F(ab′)$_2$ did not increase raft formation (data not shown). The percentage CDC of the clones to rituximab and complement is also shown. Again, high CD20 expressors are very sensitive to rituximab and the low expressors are not despite the lipid raft formation. As a negative control, CD7, expressed on CEM cells, is not completely Triton X-100–insoluble after antibody binding.

We next investigated the relationship between CD20 expression level and ADCC by incubation of CEM-CD20 clones with rituximab and effector cells. Again, clones with different CD20 expression levels were used. We found an average cell kill of 49.3 ± 14.2% (Fig. 2F). In contrast to CDC, there was no significant correlation between the number of CD20 molecules per cell and rituximab-mediated cell kill by effector cells (r^2 = 0.19; n = 13). Maximum ADCC was already achieved at the lowest MFI tested (300).

In several studies, tumor samples have been used in which the absolute number of CD20 molecules per cells (CD20-ABC) was determined (7, 11). To quantitatively compare our CD20 transgenic cells with those tumor samples, we also determined the CD20-ABC of our CD20 transgenic cells and of 6 CLL and 6 lymphoma samples. Figure 3A shows again the correlation between the absolute number of CD20 molecules per cell and

the rituximab-mediated CDC ($r^2 = 0.87$; $n = 21$). In contrast, maximum ADCC was already achieved at a CD20-ABC of 15,889 (Fig. 3B). In both figures, the range of CD20-ABC of the CLL and lymphoma samples is plotted.

To obtain additional proof of the effect of the CD20 expression level on CDC sensitivity, we transduced the CD20$^+$ Raji Burkitt's lymphoma cell line with the CD20 retroviral vector (Fig. 4A). Figure 4B shows that the additional CD20 molecules on the cell surface made the Raji cells more sensitive to rituximab-mediated CDC, because 15% more cells were killed in the presence of rituximab and human serum compared with nontransduced cells. This was also observed for CD20-transduced EBV-transformed B cells (data not shown). Thus, the CD20 expression level is of critical importance for rituximab-mediated CDC.

Next, we investigated the effect of both CDC and ADCC on rituximab-mediated cell kill on eight different CEM-CD20 clones in three independent experiments (Fig. 5A-C). These clones were selected because their CD20 MFI was within the linear range of the rituximab-mediated CDC. Figure 5D summarizes these results. Again, there was a significant correlation between the CD20 expression level and cell kill by CDC ($P = 0.002$; $r^2 = 0.82$). These results also show that the correlation of CD20 expression and rituximab-induced kill is donor (serum) independent. Again, no correlation was observed between the level of CD20 expression and rituximab-induced ADCC ($P = 0.74$; $r^2 = 0.02$).

The combined activity of CDC and ADCC correlated with the level of CD20 expression ($P < 0.02$; $r^2 = 0.62$) and was significantly higher than the activity of ADCC alone, except for two clones with a very low CD20 expression (clone 4, MFI 423; clone 17, MFI 462). Hence, no activation of complement was induced by rituximab with these clones. In addition, the combined activity of CDC and ADCC was significantly stronger than CDC alone, except for the clones with very high CD20 expression (clone 19, MFI 662; clone 21, MFI 683), because virtually all cells were killed by CDC alone. Apoptosis is a third mechanism of action described for rituximab, but we did not observe any apoptosis in this 4-hour assay or after 24 or 48 hours. In addition, binding of rituximab did also not result in growth arrest (data not shown).

These data suggested that cells not sensitive to CDC could be sensitive to ADCC and vice versa. To test this hypothesis, we first subjected a CEM-CD20 clone with high CD20 expression to CDC alone and observed 5.3 ± 0.5% cell survival (Fig. 6A). These surviving, CDC-resistant, cells were still rituximab positive as measured with an antihuman IgG1 goat antibody after 48 hours of culture (data not shown). Subsequently, the CDC-resistant cells were cultured for another 4 hours in the presence of effector cells. Only 1.0 ± 0.7 of the CDC-resistant cells survived this ADCC (Fig. 6B), whereas addition of serum had no effect. In the reciprocal experiment, the same CEM-CD20 clone was first subjected to ADCC (35.8 ± 8.5% cell survival). Human serum was then added to the remaining ADCC-resistant cells. Only 0.4 ± 0.1% of the ADCC-resistant cells survived this treatment. Together, these data show that CDC and ADCC act complementary in mediating rituximab-induced cell death. Moreover, this suggests that resistance to CDC and ADCC is mediated by separate mechanisms.

Fig. 4. Rituximab-mediated CDC assay on Raji cells. *A,* CD20$^+$ (*i*) nontransduced and (*ii*) transduced Raji cells. *B,* CDC assay on (*i*) nontransduced and (*ii*) CD20-transduced Raji cells. Dead cells were stained with PI.
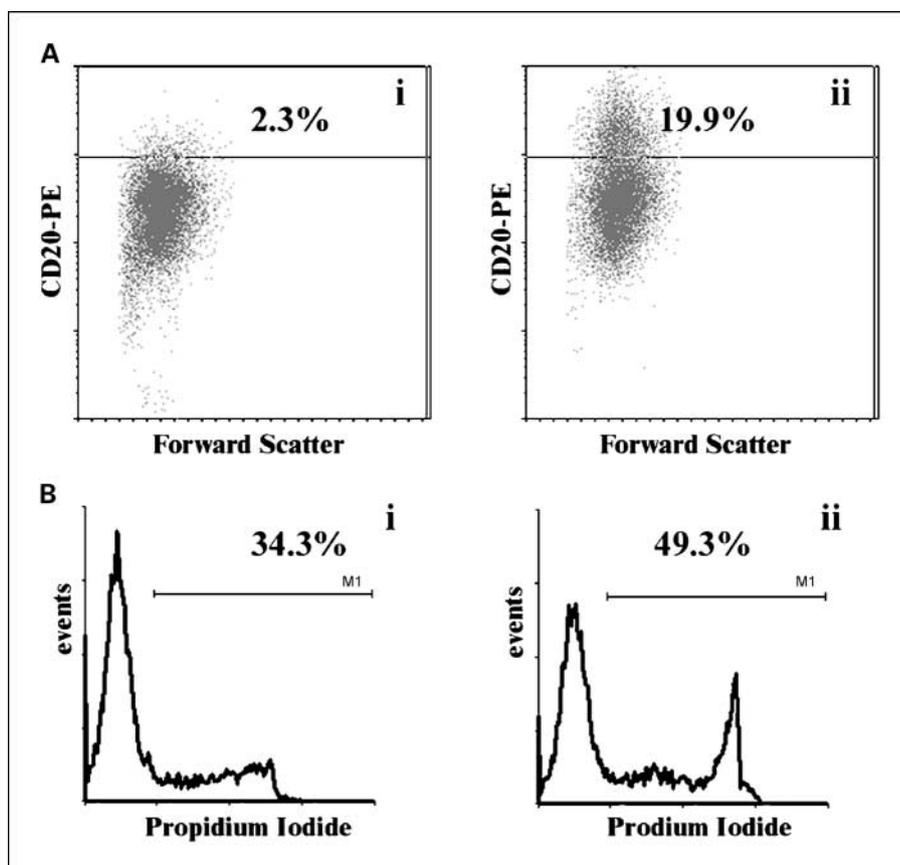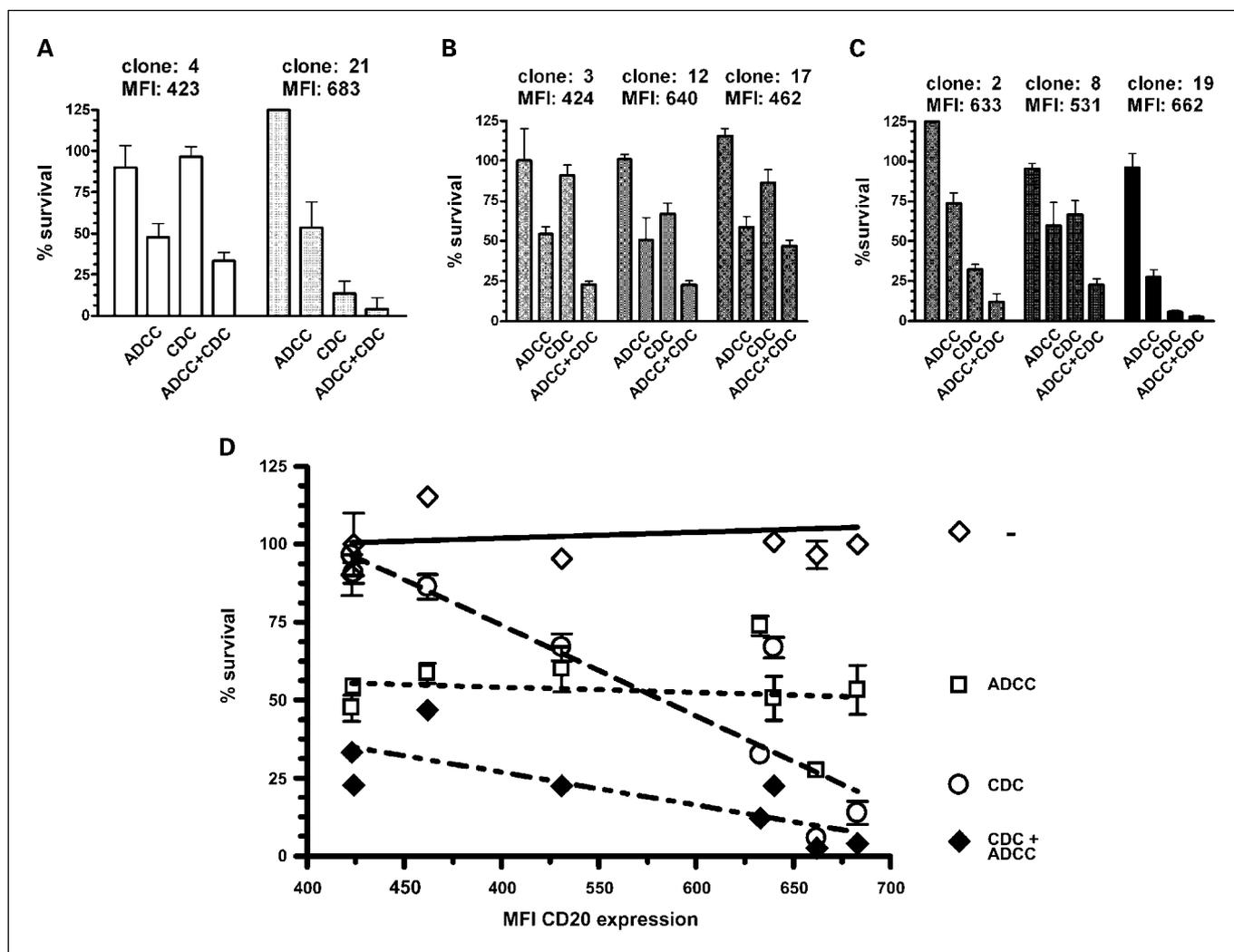
Fig. 5. Rituximab-mediated killing assays. *A* to *C,* eight individual CEM-CD20 clones with different CD20 expression levels were used and their sensitivity to rituximab-mediated CDC and ADCC was compared. Results of three different experiments with effector cells and serum from three different donors. Experiments were done in triplicate. *Columns,* mean survival; *bars,* SD. *D,* correlation between CD20 expression level on CEM-CD20 clones and sensitivity to rituximab-induced cell kill. ◇, rituximab alone without effector cells or serum (control); □, ADCC induced by rituximab and effector cells; ○, CDC induced by rituximab and complement; ♦, combination of ADCC and CDC induced by rituximab.

Discussion

Clinical data with respect to the efficacy of rituximab have shown variable response rates of different CD20^{+} malignancies (5, 22–24). The *in vivo* mechanisms of action of rituximab are not completely understood. Moreover, the mechanisms underlying the resistance to rituximab treatment are unresolved (25). The most important effector mechanisms of rituximab are activation of the complement system and the recruitment of Fc receptor (FcγR)–bearing effector cells. In addition, some reports showed that cross-linking of the CD20 molecule could lead to apoptosis and even a vaccinal effect of rituximab has been proposed (3, 26–29). It probably depends on the cellular microenvironment and the phenotype of the tumor cells of which these effector mechanisms is/are dominant *in vivo*. At this stage, there is insufficient understanding with respect to the interaction of the multiple mechanisms of action of rituximab.

The efficacy of rituximab has often been correlated with CD20 expression. In contrast to a widespread belief, this issue is still open, because the results of the various studies addressing this question are conflicting (5, 7, 10–12). Moreover, these studies only concern CDC but not ADCC or the combined contribution of CDC and ADCC to effectuate cell kill. In our experimental model, the level of CD20 expression is the only variable. The clones collectively cover a wider range of CD20 expression than the samples in other studies, which mainly involved low expressors (10–13). Our data clearly show that the sensitivity to rituximab-induced CDC correlates well with the level of CD20 expression, confirming several studies (7, 11). However, in contrast to these studies, our data indicate that the correlation is characterized by a sigmoidal rather than a linear curve. Of note, those studies mainly involved low-CD20 expressing samples and the lack of a sigmoidal relationship may have been caused by the paucity of high expressors. As a consequence, the curves did not reach a maximum plateau level. The sigmoidal shape of the curve implicates a minimum threshold number of CD20 molecules for induction of CDC. This observation may well explain the poor response of B-cell

CLL that express only low levels of CD20 (14). The effect of CD20 expression level was further strengthened by the observation that an enforced increase in CD20 expression level on Raji cells resulted in an increase in CDC susceptibility.

The activation of the complement system by CD20 antibodies has been correlated to the ability of these antibodies to translocate CD20 into lipid rafts (19). In our hands, rituximab ligation also translocates all CD20 molecules into lipid rafts independent of the number of CD20 antigens present on the cells. This creates a complex for the binding of C1q and initiates the classic pathway of the complement system. These data indicate that low CDC sensitivity of low CD20 expressors does not result from incomplete lipid raft formation. Rather, low CDC sensitivity likely results from insufficient complement fixation.

The clearly established relationship between a high CD20 expression level and high rituximab-mediated CDC in our model remains in contrast to some *in vitro* studies involving primary lymphomas (10, 12). Apparently, other biological characteristics beside CD20 expression critically affect rituximab susceptibility of these tumors even if they highly express CD20. An obvious

Fig. 6. Complementary activity of CDC and ADCC in rituximab-induced cell kill. *A,* rituximab-mediated killing of a CEM-CD20 clone with high CD20 expression by CDC, ADCC, and the combination. *Columns,* mean of experiments in triplicate; *bars,* SD. *B,* in a second experiment, the ADCC-resistant cells from the first experiment were subjected, after 48 hours of culturing, to CDC through addition of human serum (*light gray columns*). Conversely, the CDC-surviving cells from the first experiment were subjected to ADCC through addition of effector cells (*dark gray columns*).

candidate is CRP expression. Although CRP-blocking antibodies could enhance rituximab efficacy *in vitro*, CRP expression did not influence rituximab-induced CDC (7, 11, 13). In addition, neither clinical outcome nor *in vitro* CDC sensitivity correlated with CD20 expression level in a study involving rituximab sensitivity of primary follicular lymphoma cells (13). In both responding and nonresponding patients, high CD20 expression was found. However, in relation to clinical outcome, several factors, such as type of tumor and/or localization, tumor load, or tumor vascularization, play an additional role.

Although ADCC has often been implicated as a rituximab effector mechanism, only few studies have addressed the extent of cell death by ADCC thus far. These studies confirm our findings of partial ADCC-induced cell kill by rituximab *in vitro* irrespective of CD20 expression level (11, 12, 30). Various *in vivo* models have shown the significance of immune activation through FcγR for IgG (8, 31). Uchida et al. (31) showed that only the innate immune system was responsible for depleting B cells in mice. They showed that anti-CD20 mouse mAbs primarily deplete B cells through FcγR-dependent and C3-, C4-, and C1q-independent mechanisms. B cells were also cleared in natural killer cell- or T-cell-deficient mice by the different types of anti-CD20 mAbs. In contrast, B cells were not significantly eradicated in mice treated with liposome-encapsulated clodronate or in mice with CFS-1 deficiency that completely lack macrophages. Altogether, these results favor the depletion of B cells through macrophages in this model. Of note, in this study, mouse anti-CD20 mAbs were used, including the IgG1 subtype. Mouse IgG1 does not activate mouse complement (32). In contrast, rituximab, which contains a human IgG1 chain, does trigger the human complement system *in vitro* and *in vivo* (9, 33). Moreover, others have reported the essential role of complement and rituximab in a mouse model (9). Nevertheless, a pivotal role of cells expressing FcγR for the efficacy of rituximab was proven in studies with patients who differed in expression of distinct FcγRIIa and FcγRIIIa polymorphisms. FcγRIIa (only expressed by macrophages) and FcγRIIIa polymorphisms correlated with the efficiency of tumor or B-cell depletion during rituximab treatment (34–36). In addition, *in vitro* experiments confirmed the importance of polymorphisms rituximab-induced ADCC (37). In our experiments, we used total peripheral blood mononuclear cells from healthy donors stimulated for 24 hours with IL-2 and IL-12, resulting in a very strong natural killer cell activity (38). Although we did not check for FcγR polymorphisms, no significant differences between the different donors were found (data not shown; ref. 21).

The relative contribution of both CDC and ADCC on rituximab-induced cell kill has often been questioned. We here show that CDC and ADCC can act both independently and simultaneously and significantly enhance cell kill when combined. As with CDC alone, the efficiency of the combined activity of CDC and ADCC also depends on CD20 expression level. The C1q-binding site of the complement system is located within the C_H2 domain of the IgG1 chain of rituximab (39). Mutations within the C_H2 domain of rituximab resulted in impaired CDC and ADCC activity. This can be explained by the close proximity of the C1q-binding site of IgG1 to the binding site involved in binding to most FcγR subtypes (39–42). We show that CDC and ADCC act cooperatively. Thus, binding of C1q does not fully inhibit FcγR binding and vice versa. Alternatively, complement components deposited on target
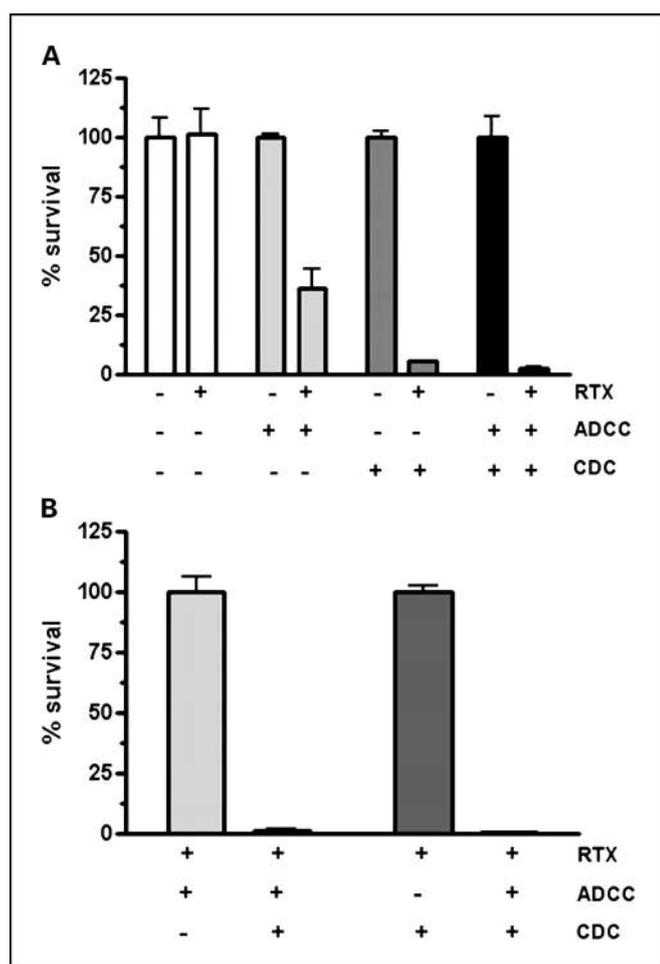
cells can act as ligands for their specific receptors on effector cells (complement-dependent cellular cytotoxicity; ref. 43). The relative contribution of CDC and ADCC *in vivo* is unclear, but complement activation has been shown to trigger the release of inflammatory cytokines and therefore the activation of effector cells (44, 45). Importantly, we show that cells resistant to CDC are still sensitive to ADCC and vice versa. The observation that (tumor-associated) CDC or (host-associated) ADCC resistance can be overcome by the complementary effector mechanism indicates that different mechanisms underlie CDC and ADCC resistance, which is most likely a reflection of the different molecular mechanisms of ADCC and CDC (induction of apoptosis and lysis, respectively).

In these studies, CD20 transgenic T cells were used and no apoptosis or growth inhibition was observed. In contrast, binding of rituximab to endogenous CD20 on B cells could lead to direct killing of the target cells and cross-linking of rituximab with secondary antibodies even increased apoptosis. Rituximab translocates the CD20 molecules into lipid rafts and reportedly activates protein tyrosine kinases of the CD20 molecule and increases intracellular Ca^{2+} concentrations, caspase activation, and subsequent cleavage of caspase substrates (26, 27, 46). At this moment, we do not know whether rituximab could induce these caspases in our CD20 transgenic T cells, but studies addressing this issue are under way.

Within this *in vitro* model, we have studied the effect of CD20 expression as the only variable and have shown a clear correlation between CD20 expression and CDC sensitivity. Because high CD20-expressing lymphoma cells are not always sensitive to rituximab *in vivo*, other variables likely affect rituximab efficacy. Nevertheless, this model shows that reduced CD20 expression leads to impaired CDC and that both CDC and ADCC can act simultaneously. To further understand the relative *in vivo* contribution of both effector mechanisms related to the CD20 expression level, these clones are currently employed in *in vivo* mouse studies. These experiments give us useful information of the importance of CD20 expression level and the efficacy of different anti-CD20 mAbs (30).

These studies add ADCC resistance to the list of potential mechanisms of rituximab resistance. Enhancing ADCC activity with, for example, IL-2 or IL-12, could enhance the susceptibility of CD20⁺ cells to FcγR-bearing effector cells (47). Alternatively, ADCC could indirectly be enhanced by changing the microenvironment of tumor cells, for example, with CpG DNA sequences. These immunostimulatory sequences induce secretion of numerous cytokines (IL-12, IL-18, IFN-α, and IFN-β) by macrophages and dendritic cells (25, 48–50). On the other hand, strategies that enhance complement fixation of anti-CD20 antibodies or that induce an up-regulation of CD20 expression, such as cytokine treatment, or the use of immune modulator agents, such as bryostatin-1, may improve CD20-targeted cell kill of low CD20-expressing cells (30, 51, 52). In addition, blocking of the CRPs CD55 or CD59 may increase the sensitivity to complement (7, 11).

References

1. Looney RJ, Anolik J, Sanz I. B cells as therapeutic targets for rheumatic diseases. Curr Opin Rheumatol 2004;16:180–5.

2. Plosker GL, Figgitt DP. Rituximab: a review of its use in non-Hodgkin's lymphoma and chronic lymphocytic leukaemia. Drugs 2003;63:803–43.

3. Cartron G, Watier H, Golay J, Solal-Celigny P. From the bench to the bedside: ways to improve rituximab efficacy. Blood 2004;104:2635–42.

4. Maloney DG, Smith B, Rose A. Rituximab: mechanism of action and resistance. Semin Oncol 2002; 29:2–9.

5. Perz J, Topaly J, Fruehauf S, Hensel M, Ho AD. Level of CD 20-expression and efficacy of rituximab treatment in patients with resistant and relapsing B-cell prolymphocytic leukemia and B-cell chronic lymphocytic leukemia. Leuk Lymphoma 2002;43: 149–51.

6. Anderson DR, Grillo-Lopez A, Varns C, Chambers KS, Hanna N. Targeted anti-cancer therapy using rituximab, a chimaeric anti-CD20 antibody (IDEC-C2B8) in the treatment of non-Hodgkin's B-cell lymphoma. Biochem Soc Trans 1997;25:705–8.

7. Bellosillo B, Villamor N, Lopez-Guillermo A, et al. Complement-mediated cell death induced by rituximab in B-cell lymphoproliferative disorders is mediated *in vitro* by a caspase-independent mechanism involving the generation of reactive oxygen species. Blood 2001;98:2771–7.

8. Clynes RA, Towers TL, Presta LG, Ravetch JV. Inhibitory Fc receptors modulate *in vivo* cytotoxicity against tumor targets. Nat Med 2000;6:443–6.

9. Di Gaetano N, Cittera E, Nota R, et al. Complement activation determines the therapeutic activity of rituximab *in vivo*. J Immunol 2003;171:1581–7.

10. Golay J, Zaffaroni L, Vaccari T, et al. Biologic response of B lymphoma cells to anti-CD20 monoclonal antibody rituximab *in vitro*: CD55 and CD59 regulate complement-mediated cell lysis. Blood 2000;95: 3900–8.

11. Golay J, Lazzari M, Facchinetti V, et al. CD20 levels determine the *in vitro* susceptibility to rituximab and complement of B-cell chronic lymphocytic leukemia: further regulation by CD55 and CD59. Blood 2001; 98:3383–9.

12. Manches O, Lui G, Chaperot L, et al. *In vitro* mechanisms of action of rituximab on primary non-Hodgkin lymphomas. Blood 2003;101:949–54.

13. Weng WK, Levy R. Expression of complement inhibitors CD46, CD55, and CD59 on tumor cells does not predict clinical outcome after rituximab treatment in follicular non-Hodgkin lymphoma. Blood 2001;98: 1352–7.

14. Almasri NM, Duque RE, Iturraspe J, Everett E, Braylan RC. Reduced expression of CD20 antigen as a characteristic marker for chronic lymphocytic leukemia. Am J Hematol 1992;40:259–63.

15. Stamenkovic I, Seed B. Analysis of two cDNA clones encoding the B lymphocyte antigen CD20 (B1, Bp35), a type III integral membrane protein. J Exp Med 1988;167:1975–80.

16. Kessels HW, van Den Boom MD, Spits H, Hooijberg E, Schumacher TN. Changing T cell specificity by retroviral T cell receptor display. Proc Natl Acad Sci U S A 2000;97:14578–83.

17. Introna M, Barbui AM, Bambacioni F, et al. Genetic modification of human T cells with CD20: a strategy to purify and lyse transduced cells with anti-CD20 antibodies. Hum Gene Ther 2000;11:611–20.

18. Ivanov R, Hol S, Aarts T, et al. UTY-specific TCR-transfer generates potential graft-versus-leukaemia effector T cells. Br J Haematol 2005;129:392–402.

19. Cragg MS, Morgan SM, Chan HT, et al. Complement-mediated lysis by anti-CD20 mAb correlates with segregation into lipid rafts. Blood 2003;101: 1045–52.

20. Jedema I, van der Werff NM, Barge RM, Willemze R, Falkenburg JH. New CFSE-based assay to determine susceptibility to lysis by cytotoxic T cells of leukemic precursor cells within a heterogeneous target cell population. Blood 2004;103:2677–82.

21. van Meerten T, Claessen MJ, Hagenbeek A, Ebeling SB. The CD20/αCD20 "suicide" system: novel vectors with improved safety and expression profiles and efficient elimination of CD20-transgenic T cells. Gene Ther 2006;13:789–97.

22. Maloney DG, Grillo-Lopez AJ, White CA, et al. IDEC-C2B8 (Rituximab) anti-CD20 monoclonal antibody therapy in patients with relapsed low-grade non-Hodgkin's lymphoma. Blood 1997;90: 2188–95.

23. McLaughlin P, Grillo-Lopez AJ, Link BK, et al. Rituximab chimeric anti-CD20 monoclonal antibody therapy for relapsed indolent lymphoma: half of patients respond to a four-dose treatment program. J Clin Oncol 1998;16:2825–33.

24. O'Brien SM, Kantarjian H, Thomas DA, et al. Rituximab dose-escalation trial in chronic lymphocytic leukemia. J Clin Oncol 2001;19:2165–70.

25. Friedberg JW. Unique toxicities and resistance mechanisms associated with monoclonal antibody therapy. Hematology (Am Soc Hematol Educ Program) 2005;329–34.

26. Shan D, Ledbetter JA, Press OW. Apoptosis of malignant human B cells by ligation of CD20 with monoclonal antibodies. Blood 1998;91:1644–52.

27. Shan D, Ledbetter JA, Press OW. Signaling events involved in anti-CD20-induced apoptosis of malignant human B cells. Cancer Immunol Immunother 2000; 48:673–83.

28. Smith MR. Rituximab (monoclonal anti-CD20 antibody): mechanisms of action and resistance. Oncogene 2003;22:7359–68.

29. Selenko N, Majdic O, Jager U, et al. Cross-priming of cytotoxic T cells promoted by apoptosis-inducing tumor cell reactive antibodies? J Clin Immunol 2002; 22:124–30.

30. Teeling JL, French RR, Cragg MS, et al. Characterization of new human CD20 monoclonal antibodies with potent cytolytic activity against non-Hodgkin lymphomas. Blood 2004;104:1793–800.

31. Uchida J, Hamaguchi Y, Oliver JA, et al. The innate mononuclear phagocyte network depletes B lymphocytes through Fc receptor-dependent mechanisms during anti-CD20 antibody immunotherapy. J Exp Med 2004;199:1659–69.

32. Klaus GG, Pepys MB, Kitajima K, Askonas BA. Activation of mouse complement by different classes of mouse antibody. Immunology 1979;38:687–95.

33. van der Kolk LE, Grillo-Lopez AJ, Baars JW, Hack CE, van Oers MH. Complement activation plays a key role in the side-effects of rituximab treatment. Br J Haematol 2001;115:807–11.

34. Anolik JH, Campbell D, Felgar RE, et al. The relationship of FcγRIIIa genotype to degree of B cell depletion by rituximab in the treatment of systemic lupus erythematosus. Arthritis Rheum 2003;48:455–9.

35. Cartron G, Dacheux L, Salles G, et al. Therapeutic activity of humanized anti-CD20 monoclonal antibody and polymorphism in IgG Fc receptor FcγRIIIa gene. Blood 2002;99:754–8.

36. Weng WK, Levy R. Two immunoglobulin G fragment C receptor polymorphisms independently predict response to rituximab in patients with follicular lymphoma. J Clin Oncol 2003;21:3940–7.

37. Dall'Ozzo S, Tartas S, Paintaud G, et al. Rituximab-dependent cytotoxicity by natural killer cells: influence of FCGR3A polymorphism on the concentration-effect relationship. Cancer Res 2004;64:4664–9.

38. Flieger D, Spengler U, Beier I, et al. Enhancement of antibody dependent cellular cytotoxicity (ADCC) by combination of cytokines. Hybridoma 1999;18:63–8.

39. Idusogie EE, Presta LG, Gazzano-Santoro H, et al. Mapping of the C1q binding site on rituxan, a chimeric antibody with a human IgG1 Fc. J Immunol 2000;164:4178–84.

40. Morgan A, Jones ND, Nesbitt AM, et al. The N-terminal end of the CH2 domain of chimeric human IgG1 anti-HLA-DR is necessary for C1q, FcγRI and FcγRIII binding. Immunology 1995;86:319–24.

41. Shields RL, Namenuk AK, Hong K, et al. High resolution mapping of the binding site on human IgG1 for FcγRI, FcγRII, FcγRIII, and FcRn and design of IgG1 variants with improved binding to the FcγR. J Biol Chem 2001;276:6591–604.

42. Sondermann P, Huber R, Oosthuizen V, Jacob U. The 3.2-A crystal structure of the human IgG1 Fc fragment-FcγRIII complex. Nature 2000;406:267–73.

43. Kennedy AD, Solga MD, Schuman TA, et al. An anti-C3b(i) mAb enhances complement activation, C3b(i) deposition, and killing of CD20⁺ cells by rituximab. Blood 2003;101:1071–9.

44. Dobrina A, Pausa M, Fischetti F, et al. Cytolytically inactive terminal complement complex causes trans-endothelial migration of polymorphonuclear leukocytes *in vitro* and *in vivo*. Blood 2002;99:185–92.

45. Frank MM, Fries LF. The role of complement in inflammation and phagocytosis. Immunol Today 1991;12:322–6.

46. Deans JP, Li H, Polyak MJ. CD20-mediated apoptosis: signalling through lipid rafts. Immunology 2002;107:176–82.

47. Gluck WL, Hurst D, Yuen A, et al. Phase I studies of interleukin (IL)-2 and rituximab in B-cell non-Hodgkin's lymphoma: IL-2 mediated natural killer cell expansion correlations with clinical response. Clin Cancer Res 2004;10:2253–64.

48. Askew D, Chu RS, Krieg AM, Harding CV. CpG DNA induces maturation of dendritic cells with distinct effects on nascent and recycling MHC-II antigen-processing mechanisms. J Immunol 2000;165:6889–95.

49. Hacker G, Redecke V, Hacker H. Activation of the immune system by bacterial CpG-DNA. Immunology 2002;105:245–51.

50. Krieg AM. From bugs to drugs: therapeutic immunomodulation with oligodeoxynucleotides containing CpG sequences from bacterial DNA. Antisense Nucleic Acid Drug Dev 2001;11:181–8.

51. Venugopal P, Sivaraman S, Huang XK, et al. Effects of cytokines on CD20 antigen expression on tumor cells from patients with chronic lymphocytic leukemia. Leuk Res 2000;24:411–5.

52. Wojciechowski W, Li H, Marshall S, Dell'Agnola C, Espinoza-Delgado I. Enhanced expression of CD20 in human tumor B cells is controlled through ERK-dependent mechanisms. J Immunol 2005;174:7859–68.

Clinical Cancer Research

Complement-Induced Cell Death by Rituximab Depends on CD20 Expression Level and Acts Complementary to Antibody-Dependent Cellular Cytotoxicity

Tom van Meerten, Rozemarijn S. van Rijn, Samantha Hol, et al.

Updated version	Access the most recent version of this article at: http://clincancerres.aacrjournals.org/content/12/13/4027

Cited articles	This article cites 51 articles, 28 of which you can access for free at: http://clincancerres.aacrjournals.org/content/12/13/4027.full#ref-list-1
Citing articles	This article has been cited by 36 HighWire-hosted articles. Access the articles at: http://clincancerres.aacrjournals.org/content/12/13/4027.full#related-urls

E-mail alerts	Sign up to receive free email-alerts related to this article or journal.
Reprints and Subscriptions	To order reprints of this article or to subscribe to the journal, contact the AACR Publications Department at pubs@aacr.org.
Permissions	To request permission to re-use all or part of this article, use this link http://clincancerres.aacrjournals.org/content/12/13/4027. Click on "Request Permissions" which will take you to the Copyright Clearance Center's (CCC) Rightslink site.